boundary condition $E_z = 0$

$$B_r(r_0) = 0 = E_\varphi(r_0) \text{ or } J_m\left(\sqrt{\gamma^2 - k^2}\, r_0\right) = 0. \quad (76)$$

We consider now the case $m = 0$. Comparing (64), (66), (68), (71), (73), and (75) with (52)–(54) we find that the latter solution corresponds to a superposition of the TE parts of B_r and B_z and the TM part of B_φ. We use, however, only the last term giving from $rB_\varphi = \text{const}$ for the "mode" $k = 0$

$$rJ_1(\gamma r) = \text{const} \quad (77)$$

(corresponding to a waveguide with cross section $r = \text{const}$) and for $k = 1$ (TM_{01} mode) we obtain

$$rJ_1\left(\sqrt{\gamma^2 - 1}\, r\right)\cos z = \text{const} \quad (78)$$

which describes the surfaces on which $B_r = E_\varphi = 0$ and into which metallic walls may be inserted without disturbing the field patterns.

References

[1] F. Cap and R. Deutsch, "Toroidal resonators for electromagnetic waves," *IEEE Trans. Microwave Theory Tech.*, vol. MTT-26, pp. 478–486, July 1978.

[2] ____, "Toroidal resonators for electromagnetic waves," *IEEE Trans. Microwave Theory Tech.*, vol MTT-28, pp. 700–703, July 1980.

[3] J. Zagrodzinski, *J. Phys. A: Math. Gen.* vol. 10, pp. 823–831, 1977.

[4] F. Cap, "Some remarks on toroidal problems," *Beitr. Plasmaphys.* vol. 18, no. 4, pp. 207–217, 1978.

[5] J. Jäger and B. Schnitzer, "Characteristic values of dominant modes within an empty torus computed by mesh method," Institut für theoretische Physik, Technische Universität Graz, Rep. ITPR-80011, June 1980.

[6] D. Nielsen, "The calculation of electromagnetic field modes in toroidal cavities of rectangular cross section," Inst. Plasma Research, Stanford Univ., SU-IPR Rep. 647, Dec. 1975.

[7] S. Przezdziecki, "TE and TM fields in orthogonal coordinate systems," *Bull. Acad. Pol. Sci.* vol. 8, nr. 8, pp. 429–436, 1960.

[8] *American Institute of Physics Handbook*, New York: McGraw-Hill, various editions.

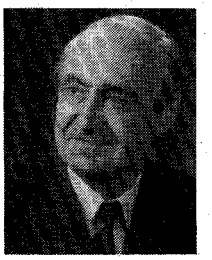

Ferdinand Cap was born in 1924 near Vienna, Austria. He studied physics, mathematics, and chemistry from 1942–1946 at the University of Vienna, Vienna, Austria.

He became a Lecturer at the University of Innsbruck, Innsbruck, Austria, in 1949 after a stay at the Zürich Technical University. He was promoted to Assistant Professor in 1955, Associate Professor with tenure in 1957, and Full Professor in 1960. In 1967 he was Guest Professor for plasma physics in New York. In 1971 he became a Senior Research Associate of NASA at Goddard Space Center and in 1979 he was a visitor at the Princeton Plasma Physics Laboratory. For 10 years he was Austria's Scientific Representative at the UN in New York. He has published more than 100 papers in physics and several textbooks about nuclear reactors and plasma physics.

Analysis and Design of TE_{11}-to-HE_{11} Corrugated Cylindrical Waveguide Mode Converters

GRAEME L. JAMES

Abstract—**A theoretical parametric study is given of a TE_{11}-to-HE_{11} mode converter consisting of a section of cylindrical corrugated waveguide with varying slot depth. The analysis makes use of modal field-matching techniques to determine the scatter matrix of the mode converter from which we deduce its propagation properties. It is shown that a mode converter consisting of only five slots achieves a return loss better than 30 dB over the band $2.7 < ka < 3.8$ (where a is the internal radius of the waveguide) with the HE_{11} mode in the balanced condition at $ka = 2.9$. The predicted results are in very good agreement with experimental data.**

Manuscript received January 7, 1981; revised April 10, 1981.

The author is with the Division of Radiophysics, CSIRO, P.O. Box 76, Epping, N.S.W. 2121, Australia.

I. Introduction

IN DESIGNING corrugated horns which use a section of cylindrical corrugated waveguide at the input, it is necessary to study the transition from a smooth-walled cylindrical waveguide supporting the TE_{11} mode to a corrugated cylindrical waveguide where the HE_{11} hybrid mode is supported. With the corrugated surface represented by

0018-9480/81/1000-1059$00.75 ©1981 IEEE

an anisotropic surface impedance, the propagation behavior through an abrupt junction between smooth-walled and corrugated guides can be solved either by numerical procedures using mode-matching techniques [1], [2] or by an analytical approach using the Wiener–Hopf method [3]. Such a junction between the two guides however often yields unacceptably low return-loss values for the TE_{11} mode. To achieve better mode conversion a corrugated transition section can be used where, by gradual variation of the slot depth, the longitudinal surface reactance χ_z is made to change smoothly from zero at the smooth-walled input guide to the high value required in the corrugated output waveguide [4]. Our purpose here is to optimize the design of such a converter to achieve maximum mode conversion (i.e., minimum reflection of the TE_{11} mode) over as wide a band as possible.

One method of analysing the performance of the TE_{11}-to-HE_{11} corrugated waveguide mode converter is to assume a waveguide with smoothly varying impedance of the walls [5]. The pitch of the corrugations however must be small compared to a wavelength (particularly where the impedance is changing rapidly) before this assumption is valid. However, in our case we wish to minimize the number of slots required in the mode converter and therefore we have taken a different approach in our analysis. First we determine the individual scatter matrices for each of the changes in waveguide cross section and for each of the short lengths of waveguide separating them which go to make up the slots and flanges of the corrugated transition section. Then by progressively cascading the scatter matrices through this section we obtain an overall scatter matrix from which we can determine the propagation properties of the mode converter.

Objections to such a scheme could be the need for excessive computer time and the possibility of accumulative errors occurring in solving for the overall scatter matrix. Fortunately these difficulties do not arise since all of the integrals required in the formulation can be evaluated analytically (as shown in Section III below), and only a modest number of waveguide modes are required to achieve satisfactory convergence.

II. Formulation

The mode converter to be analysed is shown in Fig. 1(a), where, following the smooth-walled cylindrical input waveguide supporting the TE_{11} mode, there is a section containing L slots. The depth, width, and separation of these slots are to be determined from our analysis to give the optimum mode conversion to the HE_{11} mode in the corrugated output waveguide following the Lth slot. As mentioned above, we consider each change in waveguide cross section in isolation (Fig. 1(b)) to determine its scatter matrix. Since the waveguide discontinuity problem as shown in Fig. 1(b) has been solved in [6]–[8] using mode-matching methods, we shall only briefly describe the procedure here before giving the scatter matrix for the junction between two circular waveguides.

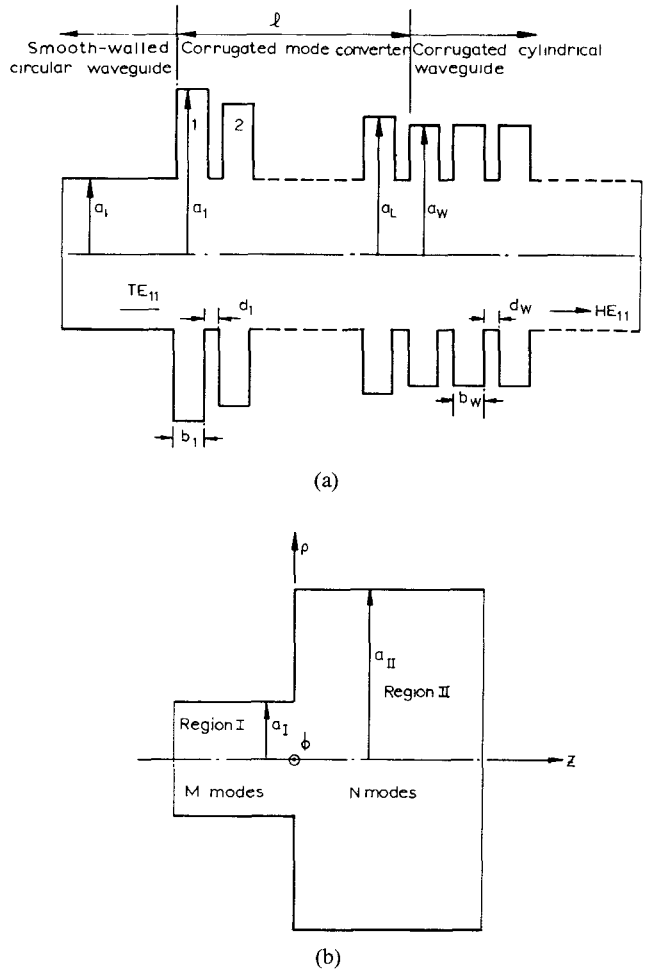

Fig. 1. Cross-sectional view of circular waveguides. (a) Corrugated mode converter section at the junction between a smooth-walled and corrugated waveguide. (b) Junction between two smooth-walled waveguides of differing radius.

In region I of Fig. 1(b) let the transverse field $\underline{E}_I$, $\underline{H}_I$ at $z=0$ be represented by the modal solution

$$\underline{E}_I = \sum_{m=1}^{M} (A_{mI} + B_{mI})\underline{e}_{mI}$$

$$\underline{H}_I = \sum_{m=1}^{M} (A_{mI} - B_{mI})\underline{h}_{mI} \tag{1}$$

where $\underline{e}_{mI}$, $\underline{h}_{mI}$ are transverse modal fields (to be described in Section III) and A_{mI}, B_{mI} are the forward and reflected modal coefficients to be determined. The upper limit M is to be made sufficiently large to ensure convergence.

Similarly for region II we have the transverse field at $z=0$ given by

$$\underline{E}_{II} = \sum_{n=1}^{N} (A_{nII} + B_{nII})\underline{e}_{nII}$$

$$\underline{H}_{II} = \sum_{n=1}^{N} (A_{nII} - B_{nII})\underline{h}_{nII} \tag{2}$$

where A_{nII}, B_{nII} are the forward and reflected modal coeffi-

cients looking *into* the junction at $z=0$.

Let s_{I} (s_{II}) be the cross-sectional area of the waveguide of radius a_{I} (a_{II}). Making use of the orthogonality of the waveguide modes, the continuity of fields over s_{I}, and the boundary conditions over $s_{\mathrm{II}}-s_{\mathrm{I}}$ (assuming that $s_{\mathrm{II}} \geqslant s_{\mathrm{I}}$), we obtain the following pair of simultaneous matrix equations

$$\underline{\underline{P}}[\underline{\underline{A}}_{\mathrm{I}}+\underline{\underline{B}}_{\mathrm{I}}]=\underline{\underline{Q}}[\underline{\underline{A}}_{\mathrm{II}}+\underline{\underline{B}}_{\mathrm{II}}]$$

$$\underline{\underline{P}}^{T}[\underline{\underline{B}}_{\mathrm{II}}-\underline{\underline{A}}_{\mathrm{II}}]=\underline{\underline{R}}[\underline{\underline{A}}_{\mathrm{I}}-\underline{\underline{B}}_{\mathrm{I}}] \tag{3}$$

where $\underline{\underline{A}}_{\mathrm{I}}$, $\underline{\underline{B}}_{\mathrm{I}}$ are column matrices of M elements containing the unknown modal coefficients $(A_{1\mathrm{I}} \cdots A_{M\mathrm{I}})$, $(B_{1\mathrm{I}} \cdots B_{M\mathrm{I}})$ of region I. Similarly $\underline{\underline{A}}_{\mathrm{II}}$, $\underline{\underline{B}}_{\mathrm{II}}$ are column matrices of N elements containing the unknown modal coefficients in region II. $\underline{\underline{P}}$ is an $N\times M$ matrix, $\underline{\underline{Q}}$ is an $N\times N$ diagonal matrix and $\underline{\underline{R}}$ is an $M\times M$ diagonal matrix. The elements in these last three matrices are given by

$$P_{mn}=\int_{s_{\mathrm{I}}} \underline{e}_{m\mathrm{I}}\times\underline{h}_{n\mathrm{II}}\cdot d\underline{s}$$

$$Q_{nn}=\int_{s_{\mathrm{II}}} \underline{e}_{n\mathrm{II}}\times\underline{h}_{n\mathrm{II}}\cdot d\underline{s}$$

$$R_{mm}=\int_{s_{\mathrm{I}}} \underline{e}_{m\mathrm{I}}\times\underline{h}_{m\mathrm{I}}\cdot d\underline{s}. \tag{4}$$

Rearranging (3) into the scattering matrix formulation

$$\underline{\underline{B}}=\underline{\underline{S}}\,\underline{\underline{A}} \tag{5}$$

where

$$\underline{\underline{B}}=\begin{bmatrix}\underline{\underline{B}}_{\mathrm{I}}\\ \underline{\underline{B}}_{\mathrm{II}}\end{bmatrix} \qquad \underline{\underline{A}}=\begin{bmatrix}\underline{\underline{A}}_{\mathrm{I}}\\ \underline{\underline{A}}_{\mathrm{II}}\end{bmatrix} \qquad \underline{\underline{S}}=\begin{bmatrix}\underline{\underline{S}}_{11} & \underline{\underline{S}}_{12}\\ \underline{\underline{S}}_{21} & \underline{\underline{S}}_{22}\end{bmatrix}$$

we have the scatter matrix elements given by

$$\underline{\underline{S}}_{11}=\left[\underline{\underline{R}}+\underline{\underline{P}}^{T}\underline{\underline{Q}}^{-1}\underline{\underline{P}}\right]^{-1}\left[\underline{\underline{R}}-\underline{\underline{P}}^{T}\underline{\underline{Q}}^{-1} \quad \underline{\underline{P}}\right]$$

$$\underline{\underline{S}}_{12}=2\left[\underline{\underline{R}}+\underline{\underline{P}}^{T}\underline{\underline{Q}}^{-1}\underline{\underline{P}}\right]^{-1}\underline{\underline{P}}^{T}$$

$$\underline{\underline{S}}_{21}=2\left[\underline{\underline{Q}}+\underline{\underline{P}}\,\underline{\underline{R}}^{-1}\underline{\underline{P}}^{T}\right]^{-1}\underline{\underline{P}}$$

$$\underline{\underline{S}}_{22}=-\left[\underline{\underline{Q}}+\underline{\underline{P}}\,\underline{\underline{R}}^{-1}\underline{\underline{P}}^{T}\right]^{-1}\left[\underline{\underline{Q}}-\underline{\underline{P}}\,\underline{\underline{R}}^{-1} \quad \underline{\underline{P}}^{T}\right]. \tag{6}$$

This equation gives the scattering matrix elements for transmission through a discontinuity in radius of a circular waveguide, assuming transmission is from the smaller to the larger guide. If transmission is from the larger to the smaller guide then (5) and (6) apply but with the scatter matrix now given by

$$\underline{\underline{S}}=\begin{bmatrix}\underline{\underline{S}}_{22} & \underline{\underline{S}}_{21}\\ \underline{\underline{S}}_{12} & \underline{\underline{S}}_{11}\end{bmatrix}.$$

The choice of mode ratio M/N is a crucial consideration. If this ratio is chosen incorrectly then it is possible to obtain a solution that is wrong no matter how many terms are taken or how convergent the result is. This problem of relative convergence has been extensively dealt with in [8], [9], [10] and it suffices to say that the condition $M/N=a_{\mathrm{I}}/a_{\mathrm{II}}$ (to the nearest rational number) must be satisfied if the answers are to converge to the correct values.

Between the discontinuities in waveguide cross section in Fig. 1(a) are short lengths of waveguide b_n and d_n making up the slots and flanges of the corrugated structure. We therefore need the scatter matrix of a length of waveguide. This is particularly simple: for a waveguide of length l, and taking N modes, the scatter matrix elements are $\underline{\underline{S}}_{11}=\underline{\underline{S}}_{22}=\underline{0}$, $\underline{\underline{S}}_{12}=\underline{\underline{S}}_{21}=\underline{\underline{V}}$, where $\underline{\underline{V}}$ is an $N\times N$ diagonal matrix with elements $V_{nn}=\exp(-\gamma_n l)$, where γ_n is the propagation constant of the nth mode in the waveguide.

To obtain the overall scatter matrix $\underline{\underline{S}}^{0}$ of the corrugated mode converter it is necessary to progressively cascade the scatter matrices of the discontinuities in cross section and the short lengths of waveguide as we advance through the mode converter. For example, in cascading two scatter matrices $\underline{\underline{S}}^{a}$ and $\underline{\underline{S}}^{b}$ the elements of the combined matrix $\underline{\underline{S}}$ become

$$\underline{\underline{S}}_{11}=\underline{\underline{S}}^{a}_{12}\left[\underline{\underline{I}}-\underline{\underline{S}}^{b}_{11} \quad \underline{\underline{S}}^{a}_{22}\right]^{-1}\underline{\underline{S}}^{b}_{11}\underline{\underline{S}}^{a}_{21}+\underline{\underline{S}}^{a}_{11}$$

$$\underline{\underline{S}}_{12}=\underline{\underline{S}}^{a}_{12}\left[\underline{\underline{I}}-\underline{\underline{S}}^{b}_{11} \quad \underline{\underline{S}}^{a}_{22}\right]^{-1}\underline{\underline{S}}^{b}_{12}$$

$$\underline{\underline{S}}_{21}=\underline{\underline{S}}^{b}_{21}\left[\underline{\underline{I}}-\underline{\underline{S}}^{a}_{22} \quad \underline{\underline{S}}^{b}_{11}\right]^{-1}\underline{\underline{S}}^{a}_{21}$$

$$\underline{\underline{S}}_{22}=\underline{\underline{S}}^{b}_{21}\left[\underline{\underline{I}}-\underline{\underline{S}}^{a}_{22} \quad \underline{\underline{S}}^{b}_{11}\right]^{-1}\underline{\underline{S}}^{a}_{22}\underline{\underline{S}}^{b}_{12}+\underline{\underline{S}}^{b}_{22} \tag{7}$$

where $\underline{\underline{I}}$ is a unit matrix. Thus beginning with the first discontinuity and short length of waveguide (i.e., the width of the first slot), we continue this procedure repeatedly through the mode converter until finally arriving at $\underline{\underline{S}}^{0}$.

If it is assumed that a unit strength TE_{11} mode in the smooth-walled input guide propagates towards the mode converter and that both the input and output waveguides terminate in matched loads, it follows, using the notation in (5), that

$$A_{1\mathrm{I}}=1, \qquad A_{m\mathrm{I}}=0 \text{ for } m>1 \text{ and } \underline{\underline{A}}_{\mathrm{II}}=\underline{0}.$$

Thus for the reflected modes we have $\underline{\underline{B}}_{\mathrm{I}}=\underline{\underline{S}}^{0}_{11}\underline{\underline{A}}_{\mathrm{I}}$ and for the transmitted modes $\underline{\underline{B}}_{\mathrm{II}}=\underline{\underline{S}}^{0}_{21}\underline{\underline{A}}_{\mathrm{I}}$. Finally, in designing mode converters we will optimize the return loss performance of the TE_{11} mode which, expressed in decibels, is given by $20\log B_{1\mathrm{I}}$.

III. The Waveguide Modes and Solutions to the Integrals

The exciting mode in Fig. 1(a) is the TE_{11} mode in the smooth-walled input guide, and therefore TE_{1n} and TM_{1n} modes can be excited at each discontinuity in the mode converter. In addition, if region II in Fig. 1(b) represents the corrugated output waveguide, HE_{1n} hybrid modes can be excited. For the latter case, approximating the corrugated surface by a longitudinal surface reactance χ_z normalized to the free-space impedance $\eta=\sqrt{\mu/\epsilon}$, the trans-

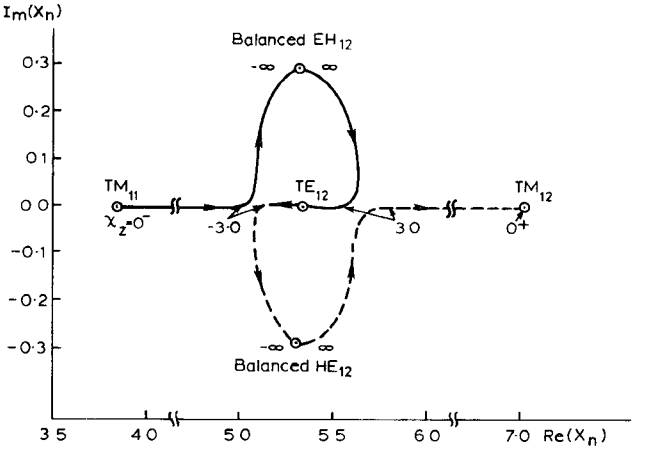

Fig. 2. Root locus of hybrid modes beyond cutoff as a function of decreasing longitudinal surface reactance χ_z of the corrugated waveguide. ——— Root locus of X_2. - - - - Root locus of X_3.

verse modal fields $\underline{e}_{n\mathrm{II}}$, $\underline{h}_{n\mathrm{II}}$ of (2) can be written as [11]

$$\frac{1}{\eta}\underline{e}_{n\mathrm{II}} = -\left[j\bar{\gamma}_n J_1'(V_n) - \Gamma_n \frac{J_1(V_n)}{V_n}\right]\underline{\hat{\rho}}\sin\phi + \left[\Gamma_n J_1'(V_n) - j\bar{\gamma}_n \frac{J_1(V_n)}{V_n}\right]\underline{\hat{\phi}}\cos\phi$$

$$\underline{h}_{n\mathrm{II}} = \left[j\Gamma_n\bar{\gamma}_n J_1'(V_n) - \frac{J_1(V_n)}{V_n}\right]\underline{\hat{\rho}}\cos\phi + \left[J_1'(V_n) - j\Gamma_n\bar{\gamma}_n \frac{J_1(V_n)}{V_n}\right]\underline{\hat{\phi}}\sin\phi \quad (8)$$

where

$$V_n = X_n\rho/a_{\mathrm{II}}$$

$$\bar{\gamma}_n = \left[(X_n/(ka_{\mathrm{II}}))^2 - 1\right]^{1/2}$$

$$\Gamma_n = \frac{\bar{\gamma}_n}{jX_n}\frac{J_1(X_n)}{J_1'(X_n)}$$

and X_n are the (complex) roots of the characteristic equation. By satisfying the longitudinal surface reactance relationship $\chi_z = jE_z(X_n)/[\eta H_\phi(X_n)]$ at the corrugated surface where the modal longitudinal electric field $E_z(X_n) = j\eta[X_n/(ka_{\mathrm{II}})]J_1(X_n)\sin\phi$, [11], we obtain the characteristic equation

$$\left\{\left[\frac{J_1(X_n)}{X_n}\right]^2\left[1-\left(\frac{X_n}{ka_{\mathrm{II}}}\right)^2\right] - \left[J_1'(X_n)\right]^2\right\}\chi_z = \frac{X_n}{ka_{\mathrm{II}}}J_1(X_n)J_1'(X_n). \quad (9)$$

If we make the assumption that only the dominant TE_1 radial waveguide mode exists in the individual slots of the corrugated output waveguide in Fig. 1(a), the solution for the surface reactance becomes (noting in this case that $a_{\mathrm{II}} = a_i$)

$$\chi_z = -\delta\frac{J_1(ka_i)Y_1(ka_w) - Y_1(ka_i)J_1(ka_w)}{J_1'(ka_i)Y_1(ka_w) - Y_1'(ka_i)J_1(ka_w)} \quad (10)$$

where δ is the ratio of slot width to pitch given by $b_w/(b_w + d_w)$. When the surface reactance $|\chi_z| \to \infty$, then $\Gamma = 1$ (for HE_{1n} modes) or -1 (for EH_{1n} modes) and the modes are said to be in the balanced hybrid condition.

Equation (8) represents hybrid modes when region II is the corrugated output waveguide. For all cases where region II is a smooth-walled guide we have $\chi_z = 0$ and (8) reduces to the expression for TE_{1n} and TM_{1n} modes. The roots X_n of (9) are then real, yielding alternatively: the roots for the TE_{1n} modes, where $J_1'(X_n) = 0$, $\Gamma = \infty$; the roots for the TM_{1n} modes, where $J_1(X_n) = 0 = \Gamma$. (With $\chi_z = 0$ equation (8) also gives the expressions for $\underline{e}_{m\mathrm{I}}$ and $\underline{h}_{m\mathrm{I}}$ in region I of Fig. 1(b) simply by replacing a_{II} with a_{I}.)

At this juncture it is worth noting the interesting behavior of the root locus of X_n with change in the surface reactance χ_z when the mode is beyond cutoff. An example of the first two cutoff modes is shown in Fig. 2, where $ka_i = 3$, and consequently only the dominant TE_{11} or HE_{11} mode can propagate in the waveguide. When $\chi_z = 0$ the cutoff modes corresponding to the roots X_2 and X_3 are the TM_{11} and TE_{12} modes, respectively. As χ_z decreases from zero in value we see from Fig. 2 that the locus of X_2 moves rapidly along the real axis while the locus of X_3 moves slowly along the real axis in the opposite direction. As χ_z decreases further there is a point (dependent on the value of ka_i) where both roots rapidly acquire an imaginary component but with opposite signs. When the balanced hybrid mode condition is reached (where $|\chi_z| = \infty$) the locus of $X_2(X_3)$ is at the root of the balanced EH_{12} (HE_{12}) mode. As noted previously, for balanced hybrid conditions [2] these modal roots form a complex conjugate pair.

When χ_z decreases from $+\infty$ the root loci behave in a similar fashion, as seen in the figure. If the value of ka_i is increased the imaginary components of the roots decrease until cutoff is reached, when the balanced EH_{12} and HE_{12} form a degenerate pair at the value of the TE_{12} root. As ka_i increases further the root loci of X_2 and X_3 move in opposite directions along the real axis. (Only the first two cutoff modes have been discussed here, but note that the root loci of higher order hybrid modes behave similarly.)

Returning now to the transverse modal fields given by

(8), we find that the integrals in (4) required for the scatter matrix formulation can be evaluated analytically by making use of known solutions to integrals containing Bessel functions [12]. In region I of Fig. 1(b), where TE_{1m} and TM_{1m} modes can be excited, let $X_{m\mathrm{I}}$ represent the roots of (9) (with $\chi_z=0$), and for region II, where the more general HE_{1n} and EH_{1n} modes can be excited (depending on the value of χ_z), let $X_{n\mathrm{II}}$ represent the roots of (9). With these parameters the evaluation of the integrals in (4) becomes

$$\left.\begin{aligned} P_{mn}&=\eta\pi J_1(X_{m\mathrm{I}})\left|\frac{J_1(X_{n\mathrm{II}}a_{\mathrm{I}}/a_{\mathrm{II}})}{(X_{m\mathrm{I}}/a_{\mathrm{I}})(X_{n\mathrm{II}}/a_{\mathrm{II}})}-\frac{j\Gamma_n\bar{\gamma}_nX_{m\mathrm{I}}J_1'(X_{n\mathrm{II}}a_{\mathrm{I}}/a_{\mathrm{II}})}{(X_{m\mathrm{I}}/a_{\mathrm{I}})^2-(X_{n\mathrm{II}}/a_{\mathrm{II}})^2}\right|, \qquad m=1,3,5,\cdots\\ P_{mn}&=\frac{j\eta\pi\bar{\gamma}_mX_{n\mathrm{II}}a_{\mathrm{I}}/a_{\mathrm{II}}\cdot J_0(X_{m\mathrm{I}})J_1(X_{n\mathrm{II}}a_{\mathrm{I}}/a_{\mathrm{II}})}{(X_{m\mathrm{I}}/a_{\mathrm{I}})^2-(X_{n\mathrm{II}}/a_{\mathrm{II}})^2}, \qquad m=2,4,6,\cdots \end{aligned}\right\} \tag{11}$$

$$Q_{nn}=\frac{\eta\pi}{(X_{n\mathrm{II}}/a_{\mathrm{II}})^2}\cdot\left\{J_1^2(X_{n\mathrm{II}})\left[\Gamma_n(1-\bar{\gamma}_n^2)-\tfrac{1}{2}\bar{\gamma}_n(1+\Gamma_n^2)(X_{n\mathrm{II}}^2-2)\right]-\tfrac{1}{2}j\bar{\gamma}_nX_{n\mathrm{II}}^2(1+\Gamma_n^2)J_0^2(X_{n\mathrm{II}})\right\} \tag{12}$$

$$R_{mm}=-\frac{\frac{1}{2}j\eta\pi\bar{\gamma}_m}{(X_{m\mathrm{I}}/a_{\mathrm{I}})^2}\begin{Bmatrix}(X_{m\mathrm{I}}^2-1) & J_1^2(X_{m\mathrm{I}})\\ X_{m\mathrm{I}}^2 & J_0^2(X_{m\mathrm{I}})\end{Bmatrix}, \qquad \begin{matrix}m=1,3,5,\cdots\\ m=2,4,6,\cdots\end{matrix}\Big\}. \tag{13}$$

For the corrugated output waveguide there exists the possibility of the EH_1 slow wave mode being excited if $\chi_z>0$. For a given value of inductive surface reactance a solution of (9) exists where the root is purely imaginary, and this characterizes the slow wave. The equations above for the hybrid modes remain valid for this additional mode.

We note here that when the mode converter is followed at the output by a uniform corrugated waveguide (as in Fig. 1(a)) a discrepancy occurs in calculating the return loss; this is caused by the surface having been approximated by the longitudinal surface reactance χ_z and by the further approximation of this impedance by (10) above. The problem arises when some of the slots and flanges of the corrugated output waveguide are incorporated into the analysis of the mode converter section. If the surface reactance χ_z accurately describes the corrugated output waveguide, then the calculated return loss should be independent of the number of slots and flanges of the corrugated waveguide included in the transition section. Because of the approximations however some variation in calculated return loss occurs, and in the results quoted below we have given the "worst case" values obtained when calculating the return loss with part of the corrugated output-waveguide structure included in the mode converter section.

IV. Theoretical Performance

The purpose of the mode converter is to provide a smooth change in χ_z from zero at the input waveguide supporting the TE_{11} mode to a large value to match the corrugated output waveguide designed to support the HE_{11} mode. This mode is balanced at a frequency f_0, chosen to be near the center of the waveguide band (where typically $ka_t=2.9$). Using a corrugated structure the surface impedance can be altered by changing the slot depth (starting either from zero or a half-guide wavelength at a given design frequency f_i at the input to the converter), varying the ratio of slot width to pitch, or a combination of both.

Fig. 3 shows computed performance for a number of these cases where the mode converters have seven slots. At the frequency f_0 with $ka_t=2.9$, the normalized slot radius ka_w in the output waveguide is 4.7 (see Fig. 1(a)) to give, ideally, $|\chi_z|=\infty$. The corrugated output waveguide pitch $p(=b_w+d_w)$ is $0.1\,\lambda_0$ and $\delta=0.75$.

Without a mode converter the return loss of the TE_{11} mode is shown by curve (*i*) in Fig. 3. Curve (*ii*) shows the return loss computed for the case where χ_z increases from zero through the use of a mode converter in which the slot depths increase linearly from zero to the slot depth of the output waveguide. It is seen that almost total reflection occurs over the waveguide band in this case. This is caused by unwanted slow waves generated in the transition section by the inductive surface reactance created when the slot depths increase from zero. If the slot depths decrease from $\lambda_t/2$ at the input, slow waves will not, in general, be excited, provided the frequency f_i is chosen to avoid the slow wave region at the higher frequencies of operation where the slots become increasingly inductive, see [4]. The resultant match achieved for this case is shown by curve (*iii*) with $f_i=f_0$. Finally, when the slot depth is constant and δ increases from a small value at the input of the converter to a value of 0.75 to match the corrugated output waveguide, it is seen from curve (*iv*) that little improvement in the return loss performance is achieved by the insertion of the mode converter.

From these results it is evident that the use of slots of decreasing depth offers the most potential for effective mode conversion from TE_{11} to a HE_{11} hybrid mode. (In fact, this practice has been used for some time in the construction of feed horns at the CSIRO Division of Radiophysics and elsewhere.) Some of the factors to be considered in designing such a mode converter include the number of slots required, the depth of the input slot, the rate at which the slot depth varies, and the effect of pitch and the ratio of width to pitch in the output waveguide. It is also desirable that the mode converter be capable of operating over a wide bandwidth.

An extensive theoretical investigation was undertaken to consider all of these factors. From this study it was found that five slots were necessary to achieve effective mode

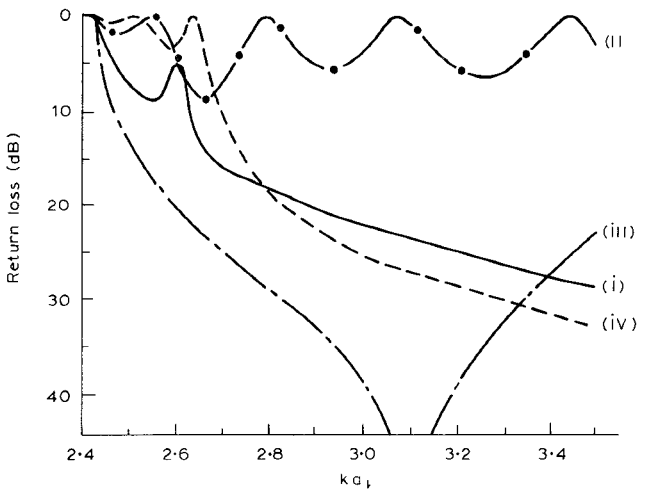

Fig. 3. Theoretical return loss of a seven-slot corrugated converter section placed between a smooth-walled and corrugated waveguide. (*i*) Return loss without the converter section. (*ii*) Converter with slot depths increasing from zero. (*iii*) Converter with decreasing slot depths, beginning with $\lambda_0/2$ at the input (f_0 is the center frequency where $ka_t = 2.9$). (*iv*) Converter with constant slot depth but with variable δ.

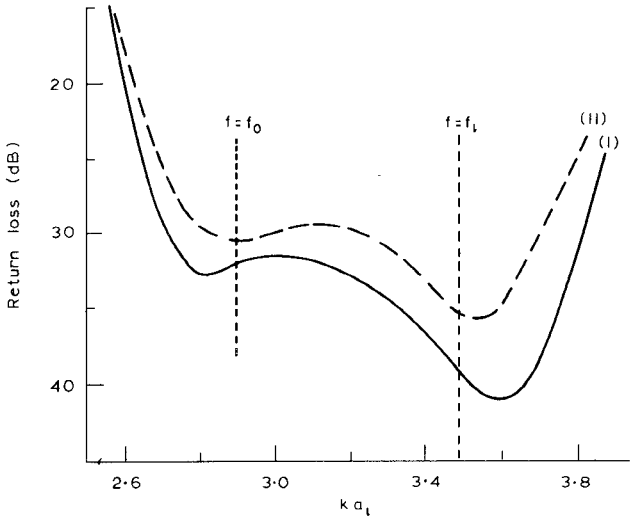

Fig. 4. Theoretical return loss of the five-slot TE_{11}-to-HE_{11} mode converters described in Table I.

conversion. The total length l of the converter containing these slots and the depth of the first slot were found to be critical. Increasing the number of slots beyond five and having moderate variation in slot width, pitch and δ (provided the coverter length l remained unchanged from its optimum value) had negligible effect on performance. A linear variation of slot depth along the transition was assumed since other variations, when tried, gave little or no improvement.

In specifying mode converter details it is not possible to consider all cases within the confines of this paper. Instead we have chosen typical smooth-walled and corrugated waveguide dimensions. As for the example given in Fig. 3, we have assumed $ka_t = 2.9$ at the nominal waveguide-band center frequency f_0. With this value, the corrugated output

TABLE I
COMPUTED PARAMETERS FOR TWO OPTIMIZED FIVE-SLOT TE_{11}-TO-HE_{11} MODE CONVERTERS, EXPRESSED IN TERMS OF THE DESIGN FREQUENCY f_0 WHERE ka_t IS 2.9 (SEE FIG. 1(a)) (THE CORRUGATED OUTPUT WAVEGUIDE HAS A PITCH OF $0.1\lambda_0$ IN CASE (i) AND $0.2\lambda_0$ IN CASE (ii))

n	Slot radius (ka_n) cases (i) & (ii)	Slot width (kb_n) (i)	Slot width (kb_n) (ii)	Flange width (kd_n) (i)	Flange width (kd_n) (ii)
0	2.90				
1	5.50	0.47	0.94	0.32	0.64
2	5.34	0.47	0.94	0.26	0.52
3	5.18	0.47	0.94	0.22	0.44
4	5.02	0.47	0.94	0.19	0.38
5	4.86	0.47	0.94	0.16	0.32
w	4.70	0.47	0.94	0.16	0.32

waveguide outer radius ka_w was 4.7 at f_0, while δ was fixed at 0.75. Two values of pitch p of the output waveguide were considered: $p = 0.1\lambda_0$ and $0.2\lambda_0$ (cases (*i*) and (*ii*)). Optimum results were obtained when the depth of the first slot of the converter was $\lambda_t/2$ at a frequency f_t corresponding to $ka_t = 3.48$. The converter length kl was found to be 3.5 at $f = f_0$ for case (*i*) and 7.0 at $f = f_0$ for case (*ii*).[1] The details of the five-slot optimum mode converter for these two cases are given in Table I. To facilitate manufacture, all of the slots in the converter have the same width as the slots in the corrugated output waveguide. Consequently, to optimize the length l the flange width was varied linearly, corresponding to a variation of δ from 0.6 to 0.75 along the converter.

Fig. 4 shows the computed TE_{11} mode return loss for both mode converters detailed in Table I. It is seen that a high value of return loss (particularly for case (*i*)) is achieved over a reasonable bandwidth. Unfortunately it does not appear to be possible to improve any further the low-frequency performance of this type of cylindrical corrugated-waveguide converter.

V. EXPERIMENTAL RESULTS

To test the validity of the theoretical development given above, a number of experiments were performed to measure the return loss of a circular waveguide system consisting of a corrugated waveguide section placed between two smooth-walled waveguides. (This avoids the practical problem of achieving a well-matched terminated corrugated waveguide.) The dimensions of the slots and flanges in the corrugated section could be varied. Preceding the input waveguide was a circular-to-rectangular waveguide transi-

[1]It must not be inferred from this result that a linear relationship always exists between kl and the value of the output waveguide pitch. This was found not to be the case in general.

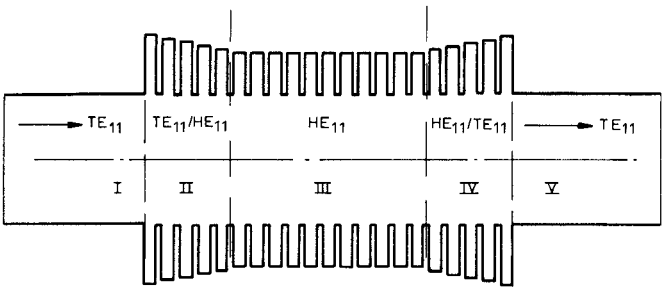

(a)

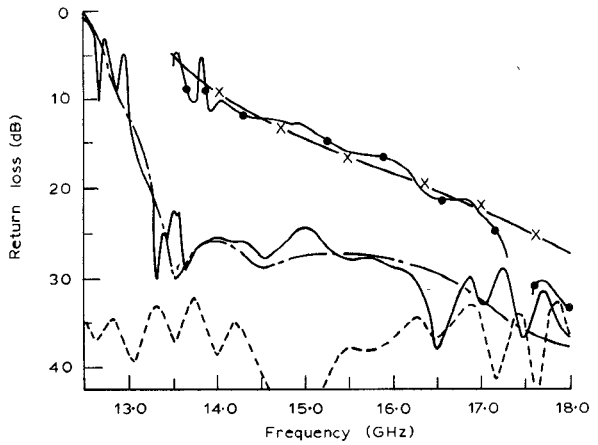

(b)

Fig. 5. Experiment to assess the performance of the optimized converter given by case (*i*) in Table I. (a) Cross-sectional view of the waveguide system. (b) Return loss performance: ——— Measured with waveguide as shown in (a). — - — Theory with waveguide as shown in (a). —●— Measured with mode converters II and IV removed. —×— Theory with mode converters II and IV removed. - - - - Measured return loss of loaded circular waveguide without the corrugated sections II, III, and IV.

tion section to enable the return loss to be measured using standard *X*-band or *Ku*-band rectangular waveguide components. The examples tested ranged from single slots or flanges of various dimensions up to a 22-slot unit. For the latter case the theoretical calculation required the cascading of 87 scatter matrices at each frequency for which the return loss was calculated. Including in the analysis up to 12 modes in the input waveguide sufficed to produce excellent agreement between theory and experiment in all cases, particularly when the return loss was substantially lower than the inherent return loss in the experimental setup, which was typically ≥ 35 dB, except at the upper edge of the band, where it decreased to around 30 dB.

In the examples shown in Fig. 4 the high value of the predicted return loss makes it difficult to verify the performance experimentally. As an attempt to assess the performance of these optimized converters, it was decided to use the following experimental technique. Two identical mode converters with parameters as given for case (*i*) in Table I were constructed to operate with 15 GHz as the design frequency f_0. We also had a short section (11 slots) of uniform corrugated waveguide accurately machined. These units were connected between the two smooth-walled circular waveguides I and V as shown in Fig. 5(a) to give double mode-conversion, viz., TE_{11} to HE_{11} back to TE_{11}. The output circular waveguide V was loaded by a long wooden load and the return loss of the input TE_{11} mode was measured over a band extending ± 20 percent about the center frequency. A similar measurement was made with the two mode converters (II and IV in Fig. 5(a)) removed. The results are shown in Fig. 5(b). Although there will be interference between the two mode converters in the first measurement and between the smooth-to-corrugated waveguide junctions in the second measurement, the pair of results at least give a qualitative measure of the effectiveness of the five-slot mode converter. The results show that the mode converter gives the predicted substantial improvement in the match. (To avoid confusion between the curves we have not plotted the results below 13.5 GHz for the case where the mode converters are absent.) Agreement between theory and experiment is generally very good, except at the upper end of the band, where the results are confused by the level of the inherent return loss of the experimental setup.

VI. Conclusion

An extensive theoretical investigation has been presented, with experimental verification, of a TE_{11}-to-HE_{11} mode converter consisting of a section of corrugated cylindrical waveguide with varying slot depths. The approach used was to evaluate by modal field-matching techniques the overall scatter matrix of the mode converter from which the transmission properties of the converter could be determined. It was found that a mode converter consisting of only five slots achieved a return loss of >30 dB over the band $2.7 < ka_t < 3.8$.

Acknowledgment

The author is indebted to B. MacA. Thomas for many useful discussions, to K. J. Greene, who performed the measurements, and to K. J. Hodgson for the machining of the corrugated waveguide sections.

References

[1] P. J. B. Clarricoats and P. K. Saha, "Propagation and radiation behaviour of corrugated feeds. I. Corrugated waveguide feed," *Proc. Inst. Elec. Eng.*, vol. 118, pp. 1167–1176, 1971.

[2] D. N. Cooper, "Complex propagation coefficients and the step discontinuity in corrugated cylindrical waveguides," *Electron. Lett.*, vol. 7, pp. 135–136, 1971.

[3] V. G. Daniele, I. Montrosset, and R. S. Zich, "Wiener–Hopf solution for the junction between a smooth and a corrugated cylindrical waveguide," *Radio Sci.*, vol. 14, pp. 943–955, 1979.

[4] B. MacA. Thomas, "Mode conversion using circumferentially corrugated cylindrical waveguide," *Electron. Lett.*, vol. 8, pp. 394–396, 1972.

[5] N. P. Kerzhentseva, "Conversion of wave modes in a waveguide with smoothly varying impedance of the walls," *Radio Eng. Electron. Phys. (USSR)*, vol. 16, pp. 24–31, 1971.

[6] A. Wexler, "Solution of waveguide discontinuities by modal analysis," *IEEE Trans. Microwave Theory Tech.*, vol. MTT-15, pp. 508–517, 1967.

[7] W. J. English, "The circular waveguide step-discontinuity mode transducer," *IEEE Trans. Microwave Theory Tech.*, vol. MTT-21,

pp. 633–636, 1973.
[8] P. H. Masterman and P. J. B. Clarricoats, "Computer field-matching solution of waveguide transverse discontinuities," *Proc. Inst. Elec. Eng.*, vol. 118, pp. 51–63, 1971.
[9] R. Mittra, "Relative convergence of the solution of a doubly infinite set of equations," *J. Res. Nat. Bur. Stand., Sect. D*, vol. 67D, pp. 245–254, 1963.
[10] S. W. Lee, W. R. Jones, and J. J. Campbell, "Convergence of numerical solutions of iris-type discontinuity problems," *IEEE Trans. Microwave Theory Tech.*, vol. MTT-19, pp. 528–536, 1971.
[11] B. MacA. Thomas, "Theoretical performance of prime-focus paraboloids using cylindrical hybrid-mode feeds," *Proc. Inst. Elec. Eng.*, vol. 118, pp. 1539–1549, 1971.
[12] I. S. Gradshteyn and I. W. Ryzhik, *Tables of Integrals, Series and Products*, New York: Academic, 1965, p. 634.

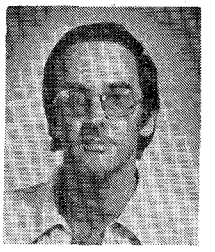

Graeme L. James was born in Dunedin, New Zealand, on September 11, 1945. He received the B.E. and Ph.D. degrees in electrical engineering from the University of Canterbury, Christchurch, New Zealand, in 1970 and 1973, respectively.

Between 1973 and 1976 he was a post-doctoral Fellow with the Department of Electrical and Electronic Engineering, Queen Mary College, London, England, where he was involved in a number of projects concerned with electromagnetic scattering and diffraction and wrote his book *Geometrical Theory of Diffraction for Electromagnetic Waves*. Since June 1976 he has been with the Division of Radiophysics, CSIRO, Sydney, Australia where he has been mainly concerned with research into high performance microwave antennas.

Surface Waves and their Relation to the Eigenfrequencies of a Circular–Cylindrical Cavity

J. V. SUBRAHMANYAM, GREGORY A. H. COWART, MUSTAFA KESKIN, HERBERT ÜBERALL, GUILLERMO C. GAUNAURD, AND EUGENIA TANGLIS

Abstract—**The eigenfrequencies of a finite-length cylindrical cavity may be interpreted as the resonances caused by the phase-matching of circumferential waves that circumnavigate the cavity along certain helical paths, and that get reflected back and forth from its top and bottom flat surfaces. In this paper, we obtain the dispersion curves of these cicumferential waves that correspond to a series of well-defined pitch angles of their helix for different values of the cylindrical cavity's length-to-radius ratio.**

I. Introduction

THE ANALYSIS of electromagnetic cavity resonators has been the subject of much previous work [1]. We shall consider here the case of a finite cylindrical cavity in a conducting medium, for which the Dirichlet boundary condition at its surface leads to transverse magnetic (TM) wave propagation, and the Neumann boundary condition leads to transverse electric (TE) wave propagation [2].

The exact expressions [2] for the finite cylindrical cavity's eigenfrequencies corresponding to the two mentioned cases are obtained in the conventional way from satisfying the appropriate boundary conditions. Consider the cavity to be filled with a uniform nondissipative medium having dielectric constant ϵ and permeability μ. With a harmonic time dependence $e^{-i\omega t}$ for the fields inside the cavity, the Maxwell equations yield

$$(\nabla^2+k^2)\boldsymbol{E}=0 \qquad (\nabla^2+k^2)\boldsymbol{B}=0 \tag{1a}$$

$$k=\mu\epsilon\omega^2/c_0^2 \tag{1b}$$

where c_0 is the speed of light *in vacuo*. The results come out in terms of standing waves with half-integer multiples of the axial wavelength along the cylinder's length and with integer multiples of azimuthal wavelength around the cylinder's circumference, while the radial boundary condition introduces the roots of the Bessel functions. If the corresponding solutions for the surface field of the cavity are transformed using the Watson–Sommerfeld method, they

Manuscript received January 9, 1981; revised April 30, 1981. The work of J. V. Subrahmanyam and H. Überall was supported by the Naval Air Systems Command under Grant AIR-310B, and the work of G. C. Gaunaurd, E. Tanglis, and H. Überall was supported by the Naval Surface Weapons Center's Independent Research Board.

J. V. Subrahmanyam, G. Cowart, and M. Keskin, are with the Department of Physics, The Catholic University of America, Washington, DC 20064.

H. Überall is with the Department of Physics, The Catholic University of America, Washington, DC 20064, and with the Naval Surface Weapons Center, White Oak, Silver Spring, MD 20910.

G. C. Gaunaurd and E. Tanglis are with the Naval Surface Weapons Center, White Oak, Silver Spring, MD 20910.

0018-9480/81/1000-1066$00.75 ©1981 IEEE